J|A|C|S
ARTICLES
Published on Web 11/22/2005

Oxygen- and Temperature-Dependent Kinetic Isotope Effects in Choline Oxidase: Correlating Reversible Hydride Transfer with Environmentally Enhanced Tunneling

Fan Fan[†] and Giovanni Gadda*[,†,‡,§]

Contribution from the Departments of Biology and Chemistry and the Center for Biotechnology and Drug Design, Georgia State University, Atlanta, Georgia 30302-4098

Received September 9, 2005; E-mail: ggadda@gsu.edu

Abstract: Choline oxidase catalyzes the flavin-linked oxidation of choline to glycine betaine, with betaine aldehyde as intermediate and oxygen as electron acceptor. Here, the effects of oxygen concentration and temperature on the kinetic isotope effects with deuterated choline have been investigated. The $^{D}(k_{cat}/K_m)$ and $^{D}k_{cat}$ values with 1,2-[$^2H_4$]-choline were pH-independent at saturating oxygen concentrations, whereas they decreased at high pH to limiting values that depended on oxygen concentration at ≤0.97 mM oxygen. The k_{cat}/K_m and k_{cat} pH profiles had similar patterns reaching plateaus at high pH. Both the limiting k_{cat}/K_m at high pH and the pK_a values were perturbed to lower values with choline and ≤0.25 mM oxygen. These data suggest that oxygen availability modulates whether the reduced enzyme-betaine aldehyde complex partitions forward to catalysis rather then reverting to the oxidized enzyme-choline alkoxide species. At saturating oxygen concentrations, the $^{D}(k_{cat}/K_m)$ was 10.6 ± 0.6 and temperature independent, and the isotope effect on the preexponential factors (A_H'/A_D') was 14 ± 3, ruling out a classical over-the-barrier behavior for hydride transfer. Similar enthalpies of activation ($\Delta H^{\ddagger}$) with values of 18 ± 2 and 18 ± 5 kJ mol^{-1} were determined with choline and 1,2-[$^2H_4$]-choline. These data suggest that the hydride transfer reaction in which choline is oxidized by choline oxidase occurs quantum mechanically within a preorganized active site, with the reactive configuration for hydride tunneling being minimally affected by environmental vibrations of the reaction coordinate other than those affecting the distance between the donor and acceptor of the hydride.

The correlation between protein structure, dynamics, and catalysis has long been a central question since the advent of transition-state theory suggested that the source of catalytic power lies in the preferential binding of the transition state, rather than the substrate, at the active site of enzymes.[1,2] The fundamental postulate of transition-state stabilization is that rate enhancement is achieved by reducing the height ($\Delta G^{\ddagger}$) of the potential energy barrier that separates the substrates from the products of the reaction.[3,4] Following the seminal work of Bell on organic reactions in solution,[5,6] experimental evidence has accumulated indicating that enzymatic reactions involving the transfer of hydrogen atoms at different oxidation states may occur via quantum mechanical tunneling through the potential energy barrier.[7−14] More recently, it became evident that many experimental observations with enzymes cannot be adequately interpreted by using Bell's semiclassical tunneling correction,[15] prompting Klinman and Scrutton to independently implicate environmentally enhanced quantum mechanical transfers of hydrogen atoms, protons, and hydride ions.[7−10,12,16−22] To date, the coupling of the reaction coordinate to environmental vibrations in the transfers of hydride ions for the oxidation of alcohols to carbonyl compounds has been investigated in enzymes that utilize zinc[8,19−21,23,24] or flavins[9,25] as cofactors. The best characterized among this group of enzymes is the zinc-dependent thermophilic alcohol dehydrogenase from *Bacillus*

[†] Department of Biology.
[‡] Department of Chemistry.
[§] Center for Biotechnology and Drug Design.

(1) Erying, H. *Chem. Rev.* **1935**, *17*, 65−77.
(2) Kraut, J. *Science* **1988**, *242*, 533−40.
(3) Jencks, W. P. *Adv. Enzymol. Relat. Areas Mol. Biol.* **1975**, *43*, 219−410.
(4) Fersht, A. *Enzyme Structure and Mechanism*, 2nd ed.; W. H. Freeman and Company: New York, 1985.
(5) Bell, R. P. *The Proton in Chemistry*, 2nd ed.; Cornell University Press: New York, 1973.
(6) Bell, R. P. *The Tunnel Effect in Chemistry*; Chapman and Hall: New York, 1980.
(7) Basran, J.; Sutcliffe, M. J.; Scrutton, N. S. *Biochemistry* **1999**, *38*, 3218−22.
(8) Tsai, S.; Klinman, J. P. *Biochemistry* **2001**, *40*, 2303−11.
(9) Seymour, S. L.; Klinman, J. P. *Biochemistry* **2002**, *41*, 8747−58.
(10) Francisco, W. A.; Knapp, M. J.; Blackburn, N. J.; Klinman, J. P. *J. Am. Chem. Soc.* **2002**, *124*, 8194−5.
(11) Maglia, G.; Allemann, R. K. *J. Am. Chem. Soc.* **2003**, *125*, 13372−3.
(12) Basran, J.; Harris, R. J.; Sutcliffe, M. J.; Scrutton, N. S. *J. Biol. Chem.* **2003**, *278*, 43973−82.
(13) Agrawal, N.; Hong, B.; Mihai, C.; Kohen, A. *Biochemistry* **2004**, *43*, 1998−2006.
(14) Sikorski, R. S.; Wang, L.; Markham, K. A.; Rajagopalan, P. T.; Benkovic, S. J.; Kohen, A. *J. Am. Chem. Soc.* **2004**, *126*, 4778−9.
(15) Kohen, A.; Klinman, J. P. *Acc. Chem. Res.* **1998**, *31*, 397−404.
(16) Basran, J.; Sutcliffe, M. J.; Scrutton, N. S. *J. Biol. Chem.* **2001**, *276*, 24581−7.
(17) Harris, R. J.; Meskys, R.; Sutcliffe, M. J.; Scrutton, N. S. *Biochemistry* **2000**, *39*, 1189−98.
(18) Knapp, M. J.; Rickert, K.; Klinman, J. P. *J. Am. Chem. Soc.* **2002**, *124*, 3865−74.
(19) Liang, Z. X.; Lee, T.; Resing, K. A.; Ahn, N. G.; Klinman, J. P. *Proc. Natl. Acad. Sci. U.S.A.* **2004**, *101*, 9556−61.
(20) Liang, Z. X.; Tsigos, I.; Bouriotis, V.; Klinman, J. P. *J. Am. Chem. Soc.* **2004**, *126*, 9500−1.
(21) Liang, Z. X.; Tsigos, I.; Lee, T.; Bouriotis, V.; Resing, K. A.; Ahn, N. G.; Klinman, J. P. *Biochemistry* **2004**, *43*, 14676−83.
(22) Kohen, A.; Cannio, R.; Bartolucci, S.; Klinman, J. P. *Nature* **1999**, *399*, 496−9.

10.1021/ja0560377 CCC: $30.25

Scheme 1. Four-Electron Oxidation of Choline Catalyzed by Choline Oxidase

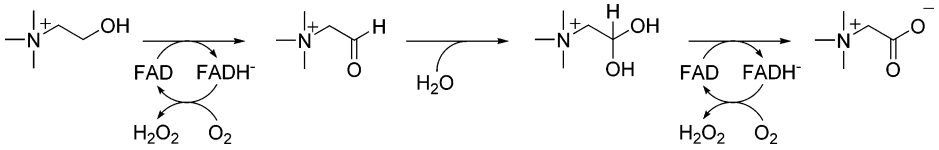

Scheme 2. Chemical Mechanism for Choline Oxidation Catalyzed by Choline Oxidase

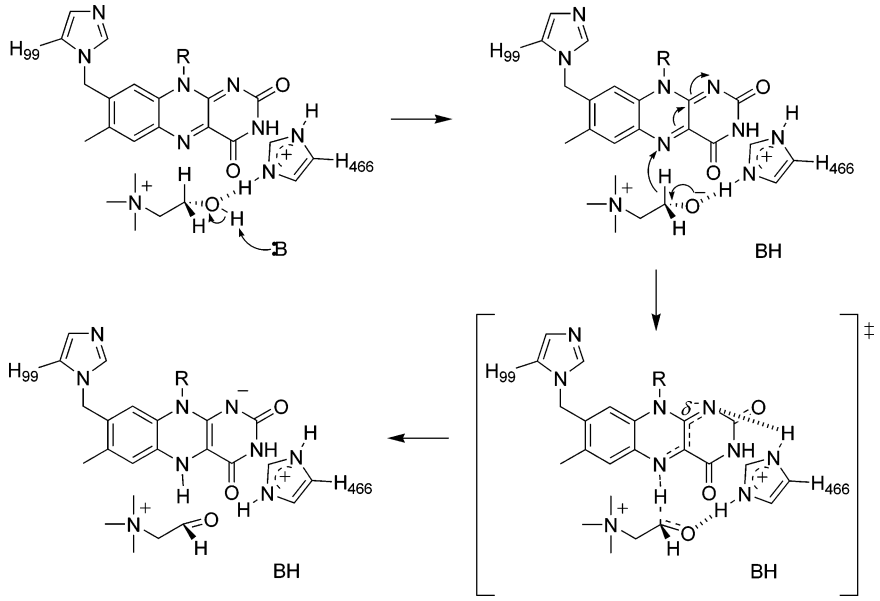

stearothermophilus, for which a temperature-dependence study of the oxidation of benzyl alcohol[19] and a protium-deuterium exchange mass spectrometry study[19,21] have provided evidence for quantum mechanical transfer of the hydride ion being coupled to protein dynamical motions. Vibrationally assisted hydride tunneling has also been demonstrated in a mutant form of horse liver alcohol dehydrogenase in which substitution of an active site amino acid residue unmasked the chemical step of hydride transfer.[24] Further support involving quantum dynamics in the hydride transfer reaction catalyzed by alcohol dehydrogenases comes from computational studies.[26] In contrast, evidence for quantum mechanical hydride transfer in flavin-dependent enzymes that oxidize alcohols is limited to mechanistic studies employing a substrate analogue on a glucose oxidase form carrying extensive surface modifications,[9,25] whereas the reaction of hydride transfer is closest to classical behavior with the wild type form of the enzyme.[9]

Choline oxidase (E.C. 1.1.3.17), a flavin-dependent enzyme that oxidizes choline, has been characterized in its biophysical, structural,[27] and mechanistic properties. The enzyme is a homodimer with a mass of 120 kDa,[28] contains covalently linked FAD in a 1:1 stoichiometry,[28] and under turnover cycles between its fully oxidized and reduced states.[29,30] The four-electron oxidation of an alcohol substrate to its corresponding acid catalyzed by choline oxidase (Scheme 1) is quite remarkable in that FAD, which can accept up to a hydride equivalent for each redox cycle,[29] is the only redox center in the enzyme.[30,31] The only other known flavin-dependent enzymes capable of catalyzing such a reaction are choline dehydrogenase[32] and thiamine oxidase,[33] for which minimal mechanistic information is available. With choline oxidase, our group has shown that the betaine aldehyde intermediate that is transiently produced during turnover with choline predominantly remains bound at the active site of the enzyme.[31] Kinetic studies have established that reduction of oxygen to hydrogen peroxide in both the oxidation reactions in which choline and betaine aldehyde are oxidized occurs via flavin-linked electron transfers in enzyme−ligand complexes.[29−31] Despite such an apparent complexity, the overall turnover with choline is limited solely by the chemical steps in which hydride ions are transferred from the choline substrate and the aldehyde intermediate to the enzyme-bound flavin.[29]

A detailed picture of the catalytic mechanism of choline oxidase has emerged from pH and kinetic isotope effects studies,[29−31,34] as well as mechanistic studies with substrate and product analogues[35] and site-directed mutants.[36] Briefly, in catalysis an active site base with a pK_a of 7.5 activates the alcohol substrate with formation of an alkoxide species,[29] which is transiently stabilized in the active site through electrostatic interaction with the imidazolium side chain of His_{466}[36] (Scheme 2). Hydride transfer from the α-carbon of the substrate to the

(23) Rubach, J. K.; Plapp, B. V. *Biochemistry* **2003**, *42*, 2907−15.
(24) Rubach, J. K.; Ramaswamy, S.; Plapp, B. V. *Biochemistry* **2001**, *40*, 12686−94.
(25) Kohen, A.; Jonsson, T.; Klinman, J. P. *Biochemistry* **1997**, *36*, 2603−11.
(26) Billeter, S. R.; Webb, S. P.; Agarwal, P. K.; Iordanov, T.; Hammes-Schiffer, S. *J. Am. Chem. Soc*. **2001**, *123*, 11262−72.
(27) The three-dimensional structure of choline oxidase is available at a resolution of 1.86 Å by X-ray crystallography (George Lountos, Fan Fan, Giovanni Gadda, and Allen M. Orville; unpublished data).
(28) Fan, F.; Ghanem, M.; Gadda, G. *Arch. Biochem. Biophys*. **2004**, *421*, 149−58.
(29) Fan, F.; Gadda, G. *J. Am. Chem. Soc*. **2005**, *127*, 2067−74.
(30) Ghanem, M.; Fan, F.; Francis, K.; Gadda, G. *Biochemistry* **2003**, *42*, 15179−88.
(31) Gadda, G. *Biochim. Biophys. Acta*. **2003**, *1646*, 112−8.
(32) Gadda, G.; McAllister-Wilkins, E. E. *Appl. Environ. Microbiol*. **2003**, *69*, 2126−32.
(33) Gomez-Moreno, C.; Edmondson, D. E. *Arch. Biochem. Biophys*. **1985**, *239*, 46.
(34) Gadda, G. *Biochim. Biophys. Acta* **2003**, *1650*, 4−9.

enzyme-bound flavin occurs from the activated alkoxide-choline species.[29] Substrate binding is mainly dictated by interactions involving the trimethylammoniun headgroup of the alcohol, with little participation of the ethyl moiety.[35] All taken together, these results suggest that the active site of choline oxidase has evolved to maximize productive binding of the alcohol substrate so that all the components of the catalytic machinery are positioned for efficient hydride transfer. This, in turn, suggests that the protein environment in the enzyme-activated substrate complex may play a significant role for promoting the transfer of the hydride ion that results in choline oxidation in the reaction catalyzed by choline oxidase. In the present study, the effects of oxygen and temperature on substrate deuterium kinetic isotope effects have been investigated to probe further the chemical mechanism of choline oxidase and the involvement of quantum tunneling in the hydride transfer reaction catalyzed by choline oxidase. The results of the studies presented herein provide further insights into the mechanism of oxidation of alcohols catalyzed by choline oxidase and, by extension, flavin-dependent enzymes that catalyze similar oxidation reactions of alcohols.

Experimental Procedures

Materials. Choline chloride was purchased from ICN. 1,2-[$^2H_4$]-Choline bromide (98%) and sodium deuterioxide (99%) were obtained from Isotec Inc. (Miamisburg, OH). Deuterium chloride (99.5%) and deuterium oxide (99.9%) were from Cambridge Isotope Co. (Andover, MA). All other reagents were of the highest purity commercially available. Recombinant choline oxidase from *A. globiformis* strain ATCC 8010 was expressed from plasmid pET/*codA1* and purified to homogeneity as described previously.[28] Fully oxidized enzyme was prepared as described previously.[35] All kinetic parameters reported in this study are expressed per active site flavin content.

Enzyme Assays. Enzyme activity was measured polarographically by monitoring initial rates of oxygen consumption with a Hansatech oxygen electrode thermostated at 10 to 45 °C. Enzyme assays were conducted in 50 mM sodium pyrophosphate, except for pH 7 and 7.5 where potassium phosphate was used. The pH of the buffered reaction mixtures varied by less than 0.07 pH units in the temperature range from 10 to 45 °C, with minimal effects on the kinetic parameters determined. The steady-state kinetic parameters at fixed oxygen conditions (0.07, 0.25, and 0.97 mM) were determined by varying the concentration of choline from 0.02 to 15 mM. Steady-state kinetics at varying concentrations of oxygen was performed by varying both oxygen (ranging from 0.04 to 1.1 mM) and choline (ranging from 0.05 to 5 mM) concentrations for each activity assay. In all cases, the assay reaction mixture was first equilibrated to the desired concentration of oxygen by bubbling the appropriate O_2/N_2 gas mixture for at least 10 min. The reactions were then started by adding 5 to 20 μL of choline oxidase at a final concentration of 0.1 to 0.4 μM into reaction mixtures with a final volume of 1 mL. Substrate deuterium kinetic isotope effects on the steady-state kinetic parameters were determined with choline and 1,2-[$^2H_4$]-choline as substrate, by alternating substrate isoptomers.

Data Analysis. Data were fit with KaleidaGraph software (Synergy Software, Reading, PA) and Enzfitter software (Biosoft, Cambridge, UK). The steady-state kinetic parameters obtained at fixed concentrations of oxygen were determined by fitting the data to the Michaelis−Menten equation for one substrate. The steady-state kinetic parameters obtained at varying concentrations of both choline and oxygen were determined by fitting the initial rate data to eqs 1 and 2, which describe steady-state kinetic mechanisms with intersecting and parallel lines, respectively. In these equations, e represents the concentration of enzyme, k_{cat} is the turnover number of the enzyme at infinite concentrations of organic substrate and oxygen, and K_a and K_b represent the Michaelis constants for the organic substrate (A) and oxygen (B), respectively. For the kinetic isotope effects, data obtained were divided into two sets, one with unlabeled substrate, and one with isotopically labeled substrate. The steady-state kinetic parameters of the two sets were determined independently with eq 1 or 2, for choline and 1,2-[$^2H_4$]-choline, respectively. The kinetic isotope effects were then determined by taking the ratios of the steady-state kinetic parameters of interest.[37] The pH dependences of the steady-state kinetic parameters were determined by fitting initial rate data to eq 3, which describes a curve with a slope of +1 and a plateau region at high pH. Y is the pH-independent value of the kinetic parameter of interest. The pH dependence of the substrate deuterium kinetic isotope effects were determined by fitting initial rate data with eq 4, where Y_L and Y_H are the limiting values at low and high pH, respectively, and K_a is the dissociation constant for the ionization of groups which are relevant to catalysis. The temperature dependences of the steady-state kinetic parameters were determined by fitting initial rate data with Eyring's equation (eq 5), where k_B and h are the Boltzmann and Planck constants, respectively. The enthalpy of activation ($\Delta H^{\ddagger}$) is calculated from the slope of the plot, whereas the entropy ($\Delta S^{\ddagger}$) is calculated from the y-intercept of the plot. The temperature dependences of the deuterium kinetic isotope effects were determined by fitting the data with Arrenhius' equation (eq 6), where A_H/A_D is the isotope effect on the preexponential factors and $[E_a(D) - E_a(H)]$ is the isotope effect on the energy of activation.

$$\frac{v}{e} = \frac{k_{cat}AB}{K_aB + K_bA + AB + K_{ia}K_b} \quad (1)$$

$$\frac{v}{e} = \frac{k_{cat}AB}{K_aB + K_bA + AB} \quad (2)$$

$$\log Y = \log\left(\frac{Y}{1 + \left(\frac{10^{-pH}}{10^{-pK_a}}\right)}\right) \quad (3)$$

$$\log Y = \log \frac{Y_L + Y_H\left(\frac{10^{-pK_a}}{10^{-pH}}\right)}{1 + \left(\frac{10^{-pK_a}}{10^{-pH}}\right)} \quad (4)$$

$$\ln(k/T) = \ln(k_B/h) + \Delta S^{\ddagger}/R - \Delta H^{\ddagger}/RT \quad (5)$$

$$\ln(\mathrm{KIE}) = \ln[A_H/A_D] - [E_a(D) - E_a(H)/RT] \quad (6)$$

Results

pH-Dependent Studies. Previous kinetic studies showed that at saturating oxygen concentrations the $^D(k_{cat}/K_m)$ and $^Dk_{cat}$ values with 1,2-[$^2H_4$]-choline as substrate for choline oxidase are pH-independent (Figure 1), consistent with cleavage of the substrate CH bond not being masked by other kinetic steps belonging to the reductive half-reaction and the overall enzyme turnover.[29] In contrast, at atmospheric oxygen concentration the $^D(k_{cat}/K_m)$ value decreases between limiting values with increasing pH, suggesting that CH bond cleavage becomes masked by some other kinetic step(s) when the enzyme is not saturated

(35) Gadda, G.; Powell, N. L.; Menon, P. *Arch. Biochem. Biophys*. **2004**, *430*, 264−73.
(36) Ghanem, M.; Gadda, G. *Biochemistry* **2005**, *44*, 893−904.

(37) As recently reported (ref 29), the quality of the fits was significantly improved when the kinetic data with deuterated choline were fit to eq 2, as illustrated for selected examples in Table S1 in the Supporting Information. Since kinetic data with choline were best fit by using eq 1, the equation $v/e = (k_{cat}AB)/\{K_a[1 + F_i(E_{k_{cat}/K_m})]B + K_bA[1 + F_i(E_{k_{cat}})] + A[1 + F_i(E_{k_{cat}})]B + K_{ia}K_b\}$ could not be used for the determination of deuterium isotope effects under steady-state conditions.

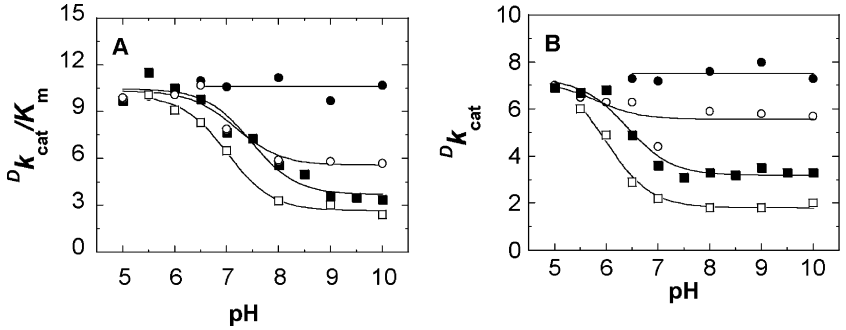

Figure 1. pH dependence of $^{D}(k_{cat}/K_m)$ and $^{D}k_{cat}$ values with 1,2-[$^2H_4$]-choline as substrate for choline oxidase at 0.07 mM (□), 0.25 mM (■), 0.97 mM (○), and saturating (●) oxygen concentrations. Activity assays of choline oxidase were performed in 50 mM buffer with choline or 1,2-[$^2H_4$]-choline as substrate, at 25 °C. Data at fixed oxygen concentrations were fit to eq 4. Data at saturating oxygen concentrations are from Fan and Gadda.[29] All data presented here are listed with their standard deviations in Table S2 in the Supporting Information.

Table 1. pH Dependence of Kinetic Isotope Effects at Different Oxygen Concentrations[a]

	$^{D}(k_{cat}/K_m)$			$^{D}k_{cat}$		
$[O_2]$, mM	Y_L[b]	Y_H[b]	pK_a	Y_L	Y_H	pK_a
∞[c]	10.6 ± 0.6	10.6 ± 0.6	n.a.[d]	7.5 ± 0.3	7.5 ± 0.3	n.a.[d]
0.97	10.3 ± 0.4	5.6 ± 0.4	7.2 ± 0.3	7.2 ± 1.0	5.5 ± 0.3	5.9 ± 0.9
0.25	10.5 ± 0.4	3.7 ± 0.4	7.5 ± 0.2	7.3 ± 0.3	3.2 ± 0.2	6.3 ± 0.1
0.07	10.1 ± 0.2	2.6 ± 0.2	7.2 ± 0.2	7.5 ± 0.6	1.8 ± 0.1	6.0 ± 0.1

[a] Conditions: 50 mM buffer, pH from 5 to 10 and 25 °C; data were fit to eq 4. [b] Y_L and Y_H are the limiting values at low and high pH, respectively. [c] Data are from ref 29. [d] n.a., not applicable.

with oxygen.[34,38] In the present study, we have followed up on those initial observations and determined the pH profiles of the $^{D}(k_{cat}/K_m)$ and $^{D}k_{cat}$ values with 1,2-[$^2H_4$]-choline as substrate for choline oxidase at three fixed concentrations of oxygen. As expected, the $^{D}(k_{cat}/K_m)$ and $^{D}k_{cat}$ values determined at 0.07, 0.25, and 0.97 mM oxygen decreased between limiting values with increasing pH (Figure 1). In all cases, the limiting $^{D}(k_{cat}/K_m)$ and $^{D}k_{cat}$ values at low pH were close to the values of 10.6 and 7.5 observed at saturating oxygen concentrations (Figure 1).[39] In contrast, the limiting $^{D}(k_{cat}/K_m)$ and $^{D}k_{cat}$ values at high pH were lower than the values determined at saturating oxygen concentrations, with the largest value observed at 0.97 mM oxygen, followed in order by those observed at 0.25 mM and 0.07 mM oxygen (Figure 1). The pK_a values defined by the $^{D}(k_{cat}/K_m)$ and $^{D}k_{cat}$ pH profiles were ∼7.5 and ∼6.0, respectively, and were independent of oxygen concentration. The limiting kinetic isotope effects at the pH extremes and the pK_a values determined from the pH profiles of the kinetic isotope effects at different oxygen concentrations are summarized in Table 1.

The pH profiles of the k_{cat}/K_m and k_{cat} with choline and 1,2-[$^2H_4$]-choline determined in this study are shown in Figure 2, along with previous data acquired at saturating oxygen concentrations.[30] Irrespective of the oxygen concentration and the isotopic composition of the substrate, the pH profiles had similar patterns with k_{cat}/K_m and k_{cat} values increasing to limiting values as the pH increased. For each substrate, the k_{cat}/K_m and k_{cat} values in the ascending limb of the curve at low pH were similar irrespective of the concentration of oxygen (Figure 2). In contrast, the limiting k_{cat}/K_m and k_{cat} values with choline at high pH were lower at concentrations of oxygen equal or less than 0.25 mM (Table 2). Interestingly, the pK_a values defined in the k_{cat}/K_m pH profiles with both substrates had similar values of ∼7.5 at all oxygen concentrations, except with choline at 0.07 and 0.25 mM oxygen where lower values were observed (Table 2). The pK_a values in the k_{cat} pH profiles spanned from 6 to 7.2, with the lowest values observed with choline at 0.07 and 0.25 mM oxygen (Table 2).

Temperature-Dependence Studies. The effect of temperature on the $^{D}(k_{cat}/K_m)$ and $^{D}k_{cat}$ values at saturating oxygen concentrations was determined to probe the involvement of quantum mechanical tunneling in the reaction of hydride transfer catalyzed by choline oxidase. Initial rates of reaction were measured at pH 8 over the temperature range from 10 to 45 °C, at varying concentrations of both the organic substrate and oxygen to avoid artifactual contributions of oxygen. The analysis of the temperature dependence of the k_{cat}/K_m and k_{cat} values according to Eyring's formalism is shown in Figure 3. Both the $\ln(k_{cat}/K_mT)$ and $\ln(k_{cat}/T)$ values increased monotonically with increasing temperature yielding similar slopes for choline and 1,2-[$^2H_4$]-choline, consistent with similar enthalpies of activation ($\Delta H^{\ddagger}$) for cleavage of the CH and CD bonds. Similar entropies of activation ($-T\Delta S^{\ddagger}$), in the range from 24 to 33 kJ mol^{-1}, were observed in both the overall turnover and the reductive half-reaction irrespective of whether the light or heavy

(38) The K_m values for oxygen when choline is used as substrate for choline oxidase range from 0.1 mM at pH 6 to 1.6 mM at pH 10 (Fan Fan and Giovanni Gadda; unpublished results). Consequently, at a concentration of oxygen of 0.25 mM, i.e., at atmospheric oxygen, the enzyme is not saturated with oxygen.

(39) For the kinetic mechanism of choline oxidase (Scheme 4), both chemical steps of oxidation (k_3 and k_7) are isotope sensitive and rate limiting for the overall turnover of the enzyme (ref 29). Consequently, while the $^{D}(k_{cat}/K_m)$ equals $^{D}k_3$, the $^{D}k_{cat}$ has a lower value according to $^{D}k_{cat} = [(^{D}k_3 + {}^{D}k_7(k_3/k_7)]/(1 + k_3/k_7)$, where $^{D}k_3$ and $^{D}k_7$ are the intrinsic isotope effect values for cleavage of the CH bonds of choline and betaine aldehyde, respectively, and k_3 and k_7 are the first-order kinetic rate constants for the chemical steps of oxidation of choline and betaine aldehyde, respectively (ref 29). In this context, the overall isotope effect for CH bond cleavage of the alcohol substrate is contributed by primary and secondary effects, allowing for the calculation of a primary isotope effect of ∼8 from the observed $^{D}(k_{cat}/K_m)$ value of ∼10.6 at saturating oxygen concentrations after accounting for an α-secondary effect of 1.24 and two β-secondary effects of 1.05 (for references, see: Cleland, W. W. In *Methods in Enzymology*; Purich, D. L., Ed.; Academic Press: New York, 1980; Vol. 64, pp 104−25. Hill, E. A.; Milosevich, S. A. *Tetrahedron Lett.* **2003**, *50*, 4553−4. Lewis, C. A., Jr.; Wolfenden, R. *Biochemistry* **1977**, *16*, 4886−90).

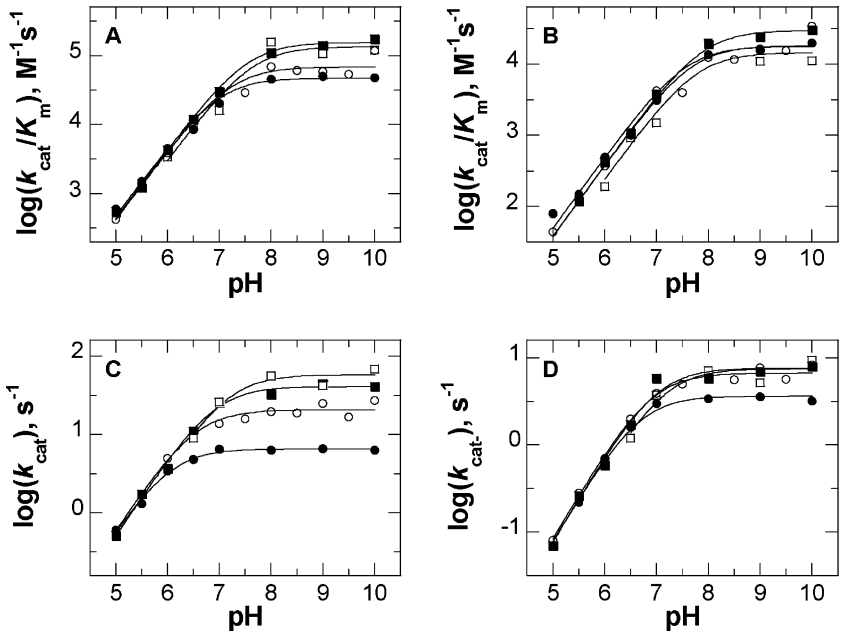

Figure 2. pH dependence of k_{cat}/K_m and k_{cat} values with either choline (panels A and C) or 1,2-[$^2H_4$]-choline (panel B and D) as substrate for choline oxidase, at 0.07 mM (●), 0.25 mM (○), and 0.97 mM (■), and saturating oxygen concentrations (□). Activity assays of choline oxidase were performed in 50 mM buffer with choline or 1,2-[$^2H_4$]-choline as substrate, at 25 °C. Data were fit to eq 3. Data at saturating oxygen concentrations are from Ghanem et al.[30] All data presented here are listed with their standard deviations in Table S2 in the Supporting Information.

Table 2. pK_a Values for Steady-State Kinetic Parameters with Choline or 1,2-[$^2H_4$]-Choline as Substrate[a]

		k_{cat}/K_m, M^{-1} s^{-1}		k_{cat}, s^{-1}	
substrate	$[O_2]$, mM	pK_a	Y^b	pK_a	Y^b
choline	∞[c]	7.6 ± 0.2	130 000 ± 30 000	7.1 ± 0.1	58 ± 8
	0.97	7.5 ± 0.1	150 000 ± 13 000	6.9 ± 0.1	41 ± 3
	0.25	7.3 ± 0.1	66 000 ± 9000	6.5 ± 0.1	21 ± 1
	0.07	7.0 ± 0.1	47 000 ± 5000	6.0 ± 0.1	6.6 ± 0.3
1,2-[$^2H_4$]-choline	∞[c]	7.8 ± 0.2	14 000 ± 5000	7.1 ± 0.2	7.5 ± 1.2
	0.97	7.5 ± 0.2	29 000 ± 6000	7.0 ± 0.1	7.6 ± 0.9
	0.25	7.6 ± 0.1	18 000 ± 3000	6.9 ± 0.1	6.7 ± 0.4
	0.07	7.6 ± 0.1	18 000 ± 3000	6.7 ± 0.1	3.6 ± 0.2

[a] Conditions: 50 mM buffer, pH from 5 to 10 and 25 °C; data were fit to eq 3. [b] *Y*, limiting value at high pH. [c] Data are from ref 29.

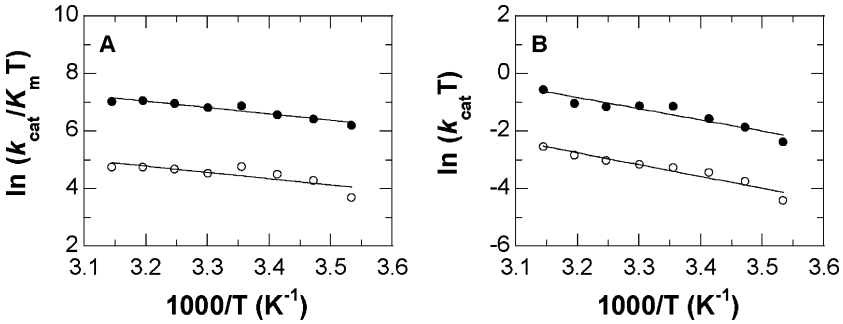

Figure 3. Temperature dependence of k_{cat}/K_m (panel A) and k_{cat} (panel B) with choline (●) or 1,2-[$^2H_4$]-choline (○) as substrate at saturating oxygen concentrations. Activity assays of choline oxidase were performed at varying concentrations of choline or 1,2-[$^2H_4$]-choline and oxygen in 50 mM sodium pyrophosphate, pH 8, in the temperature range from 10 to 45 °C. Data were fit to eq 5. All data presented here are listed with their standard deviations in Table S3 in the Supporting Information.

substrate was used (Table 3). The isotope effects on the preexponential factors (A_H'/A_D') for the k_{cat}/K_m and k_{cat} values calculated from the ratio of the *y*-intercepts of the lines in Figure 3 with choline and 1,2-[$^2H_4$]-choline[40] were, within the accuracy of the analysis, similar to the $^D(k_{cat}/K_m)$ and $^Dk_{cat}$ values previously determined at saturating oxygen concentrations and 25 °C (Table 3). Finally, similar Gibbs free energy of activations ($\Delta G^{\ddagger}$) could be calculated for CH and CD bond cleavage from the enthalpies and entropies of activations experimentally determined, for both the reductive half-reaction and the overall

(40) From the data shown in Figure 3, the preexponential factors with choline (A_H') and 1,2-[$^2H_4$]-choline (A_D') are estimated from the *y*-intercepts of the lines determined with the two substrates; the isotope effect is then the ratio (A_H'/A_D') of the preexponential factors. Since the linear fits of the two sets of data in Figure 3 have small standard deviations, the isotope effect on the preexponential factors estimated in this fashion has a small standard deviation.

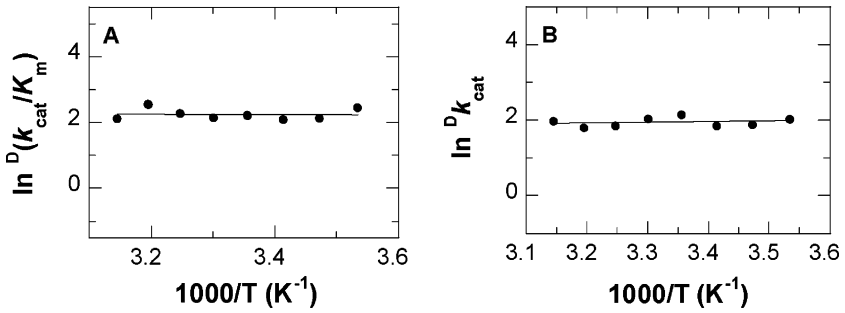

Figure 4. Temperature dependence of ${}^{D}(k_{cat}/K_m)$ and ${}^{D}k_{cat}$ values with 1,2-[$^2H_4$]-choline as substrate at saturating oxygen concentrations. Activity assays of choline oxidase were performed at varying concentrations of choline or 1,2-[$^2H_4$]-choline and oxygen in 50 mM sodium pyrophosphate, pH 8, in the temperature range from 10 to 45 °C. Data were fit to eq 6. All data presented here are listed with their standard deviations in Table S3 in the Supporting Information.

Table 3. Thermodynamic Parameters for the Reaction Catalyzed by Choline Oxidase at Saturating Oxygen Concentrations[a]

parameter	k_{cat}/K_m	k_{cat}
$\Delta H^{\ddagger}_{H}$[b], kJ mol^{-1}	18 ± 2	32 ± 6
$\Delta H^{\ddagger}_{D}$[b], kJ mol^{-1}	18 ± 5	34 ± 4
$-T\Delta S^{\ddagger}_{H}$[b], kJ mol^{-1}	24 ± 2	30 ± 5
$-T\Delta S^{\ddagger}_{D}$[b], kJ mol^{-1}	30 ± 5	33 ± 5
$\Delta G^{\ddagger}_{H}$[c], kJ mol^{-1}	42 ± 3	62 ± 8
$\Delta G^{\ddagger}_{D}$[c], kJ mol^{-1}	48 ± 7	67 ± 6
ΔE_a, kJ mol^{-1}	0.4 ± 4.2	2 ± 3
A_H'/A_D'[d]	14 ± 3	12 ± 3
KIE[e]	10.6 ± 0.6	7.5 ± 0.6

[a] Conditions: 50 mM sodium pyrophosphate, pH 8. [b] Data were calculated by using the Eyring equation (eq 5). [c] Data for 25 °C. [d] A_H'/A_D' is the ratio of the *y*-intercepts obtained by fitting the kinetic data with choline and 1,2-[$^2H_4$]-choline to the Eyring equation (eq 5). [e] KIE, kinetic isotope effects from ref 29.

turnover of the enzyme (Table 3). As illustrated in Figure 4, the analysis of ${}^{D}(k_{cat}/K_m)$ and ${}^{D}k_{cat}$ values according to Arrhenius' formalism showed that the kinetic isotope effects were temperature independent in both the reductive half-reaction and the overall turnover of the enzyme, with negligible ΔE_a values (Table 3).

Discussion

The effects of oxygen concentration and temperature on the kinetic isotope effects with deuterated choline have been investigated in this study to further characterize the reaction of alcohol oxidation catalyzed by choline oxidase. This reaction involves the transfer of a hydride from the α-carbon of an activated alkoxide form of choline to the N(5) position of the flavin cofactor[29] (step 2 in Scheme 3). The choline-alkoxide species is produced in the enzyme−substrate complex by the action of an enzymic base with a pK_a of 7.5[30,34,35] (step 1 in Scheme 3). Oxidation of the reduced flavin then occurs prior to the dissociation of the betaine aldehyde product of the reaction[30,31] (step 3 in Scheme 3). Primary deuterium kinetic isotope effects provide a direct probe of the status of the CH bond.[41] The effect of oxygen concentration on the kinetic isotope effects with deuterated choline can therefore be used to probe the reversibility of the hydride transfer reaction catalyzed by choline oxidase. The effect of temperature on the kinetic isotope effects can provide evidence on whether hydride transfer occurs quantum mechanically.[7−14,16−19,23,24,42,43]

Oxygen availability determines whether the reduced enzyme-betaine aldehyde complex partitions forward to catalysis during turnover of the enzyme with choline rather than reverting to the oxidized enzyme−choline alkoxide complex. This, in turn, establishes the reversibility of the hydride transfer reaction. Evidence for this conclusion comes from the decrease in the limiting ${}^{D}(k_{cat}/K_m)$ values with choline at high pH determined at oxygen concentrations ≤ 0.97 mM as compared to the ${}^{D}(k_{cat}/K_m)$ value determined at saturating oxygen concentrations. In the steady-state kinetic mechanism of choline oxidase,[30,31] which is summarized in Scheme 4, the apparent ${}^{D}(k_{cat}/K_m)$ value for choline is given by eq 7,[29] where 1.24 is the value for the equilibrium isotope effect for the conversion of an alcohol to an aldehyde,[44] ${}^{D}k_3$ is the intrinsic isotope effect, and C_f and C_r represent the forward and reverse commitments to catalysis, respectively. Previous pH studies on the inhibition of choline oxidase by glycine betaine[30] and with the choline analogues *N*,*N*-dimethylethanolamine and *N*-methylethanolamine as substrate for the enzyme[35] support the notion that choline is a slow substrate for the enzyme, consistent with a negligible forward commitment to catalysis.[30,35,41] Consequently, any decrease in the apparent ${}^{D}(k_{cat}/K_m)$ value must be due to the presence of a reverse commitment to catalysis, which for the kinetic mechanism of choline oxidase is given by the ratio of the rate constant for the reverse hydride transfer step (k_4) to the product of the second-order rate constant for oxygen reaction (k_5) and oxygen concentration (eq 8). Because at saturating oxygen concentrations C_r approaches zero, the resulting ${}^{D}(k_{cat}/K_m)$ value is pH-independent and approaches the value of the intrinsic kinetic isotope effect.[29] In contrast, at concentrations of oxygen in the 0.07 to 0.97 mM range, where C_r has finite values, the limiting ${}^{D}(k_{cat}/K_m)$ values at high pH will progressively decrease with decreasing oxygen concentrations, as was experimentally observed.

$$ {}^{D}\left(\frac{k_{cat}}{K_m}\right) = \frac{{}^{D}k_3 + C_f + 1.24C_r}{1 + C_f + C_r} \tag{7} $$

$$ C_r = \frac{k_4}{k_5[O_2]} \tag{8} $$

The effect of oxygen concentration on the k_{cat}/K_m pH profiles with choline provides independent support of the role of oxygen in controlling whether the reduced enzyme−betaine aldehyde

(41) Cleland, W. W. In *Isotope Effects in Chemistry and Biology*; Kohen, A., Limbach, H. H., Eds.; Taylor & Francis, CRC Press: New York, 2005; Chapter 37, pp 915−30.
(42) Bell, R. P. *Chem. Soc. Rev.* **1974**, 513−44.
(43) Hatcher, E.; Soudackov, A. V.; Hammes-Schiffer, S. *J. Am. Chem. Soc.* **2004**, *126*, 5763−75.
(44) Cleland, W. W. Measurement of isotope effect by the equilibrium perturbation technique. In *Methods in Enzymology*; Purich, D. L., Ed. Academic Press: New York, 1980; Vol. 64, pp 104−125.

Scheme 3. Reductive (1 and 2) and Oxidative (3) Half-Reactions in the Oxidation of Choline Catalyzed by Choline Oxidase

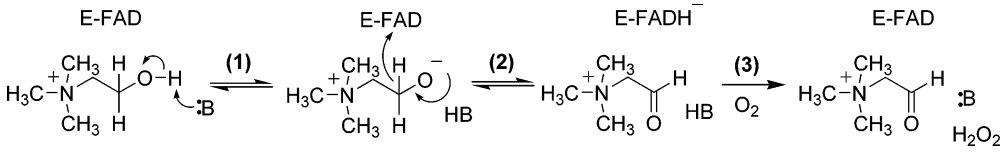

Scheme 4. Steady-State Kinetic Mechanism of Choline Oxidase[a]

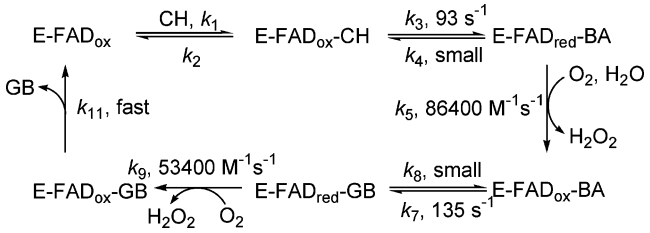

[a] Values for individual rate constants are for pH 10, where kinetic steps are pH-independent (from ref 29).

complex partitions forward to catalysis rather than reverting to the oxidized enzyme−choline alkoxide complex. The reaction of the reduced enzyme−betaine aldehyde complex with oxygen is pH-independent, as shown in a previous kinetic study.[30] This establishes that any pH effect on the k_{cat}/K_m value for choline must be ascribed to the reductive half-reaction that leads to the formation of the reduced enzyme−betaine aldehyde complex. In the kinetic mechanism of Scheme 4, the k_{cat}/K_m value for choline comprises rate constants reflecting substrate binding, k_1 and k_2, the catalytic step of choline oxidation, k_3 and k_4, and the kinetic step in which the reduced enzyme-betaine aldehyde complex is oxidized by oxygen, k_5, as illustrated in eq 9.[45] This equation predicts that at low concentrations of oxygen the pH-independent k_{cat}/K_m values and, consequently, the apparent pK_a values determined in the k_{cat}/K_m pH profiles with choline will be lower[46] than the corresponding values determined at saturating oxygen concentrations. Both these predictions are validated by the kinetic data presented here. Indeed, the pH-independent k_{cat}/K_m values with choline at high pH progressively decrease with decreasing oxygen, and the pK_a value for the group that needs to be unprotonated is perturbed to lower values when the concentration of oxygen is ≤0.25 mM.

$$\frac{k_{cat}}{K_m} = \frac{k_1 k_3}{\dfrac{k_4}{k_2 \dfrac{k_4}{k_5[O_2]}} + k_2 + k_3} \qquad (9)$$

The hydride transfer reaction in which choline is oxidized by choline oxidase occurs quantum mechanically within a highly preorganized active site. Evidence for this conclusion is provided by the temperature effects on the k_{cat}/K_m and $^D(k_{cat}/K_m)$ values with choline as substrate.[47] The large isotope effect on the preexponential factors (A_H'/A_D') determined from the temperature dependence of the k_{cat}/K_m values with choline and 1,2-[$^2H_4$]-choline, with a value of ∼14, immediately rules out a classical over-the-barrier behavior for hydride transfer, for which A_H'/A_D' values between 0.7 and 1.7 are predicted.[42] The temperature-independent $^D(k_{cat}/K_m)$ value and the enthalpies of activations ($\Delta H^{\ddagger}$) with finite values of ∼18 kJ mol^{-1} for cleavage of the CH and CD bonds do not agree with theoretical models where H and D tunnel just below the classical transition state. Indeed, such models predict that lack of temperature dependence in the kinetic isotope effect must be accompanied by a lack of temperature dependence on the reaction rates with both the light and heavy isotopes.[15,48] In contrast, the similarities in the values determined for A_H'/A_D' values for the k_{cat}/K_m values and the $^D(k_{cat}/K_m)$ value, as well as in the enthalpies of activations ($\Delta H^{\ddagger}$) for the k_{cat}/K_m values with choline and 1,2-[$^2H_4$]-choline, are consistent with environmentally enhanced tunneling of the hydride that is transferred from the choline-alkoxide species to the enzyme-bound flavin.[18,43,48] The lack of temperature dependence of the kinetic isotope effect on the k_{cat}/K_m value suggests that during the catalytic event the enzyme−substrate complex has a preorganized structure, consistent with little modulation of the tunneling probability effected

(45) Equation 9 is directly derived from the canonical expression for $k_{cat}/K_m = \{k_1k_3k_5[O_2]\}/\{k_2k_4 + k_2k_5[O_2] + k_3k_5[O_2]\}$ by dividing both numerator and denominator by $k_5[O_2]$.

(46) pK_a values determined from k_{cat}/K_m pH profiles can be perturbed outward from their intrinsic values if the substrate has a significant commitment to catalysis (ref 41). The degree to which the pK_a value is perturbed is given by $\Delta pK_a = \log(1 + C_x)$ (eq 10), where ΔpK_a is the difference between the pK_a value seen in the k_{cat}/K_m pH profile and the intrinsic pK_a value, and C_x is generally intended as the external forward commitment to catalysis, i.e., the ratio of the rate constant for catalysis to the rate constant for dissociation of the substrate from the enzyme−substrate complex (ref 41). Choline being a slow substrate for choline oxidase (ref 35) immediately rules out the presence of a forward commitment to catalysis. Equation 9 establishes a direct correlation between the reverse commitment to catalysis (C_r) and the magnitude of the k_{cat}/K_m value with choline, thereby suggesting that with choline as substrate for the enzyme the pK_a value is perturbed due to C_r. With deuterated choline, C_r is too small to yield observable perturbations of the k_{cat}/K_m pH profiles, as illustrated below. From the ΔpK_a of 0.5 units determined with choline at 0.07 mM oxygen, by using eq 10 and a value of 7.5 for the intrinsic pK_a for the group that must be unprotonated in the reductive half-reaction (ref 29), values in the range from 1 to 3 can be estimated for C_r. By using eq 8 and a value of 8×10^4 M^{-1} s^{-1} for k_5 (ref 29), one therefore estimates the rate for the reverse of the hydride transfer step with choline (k_4) to be between 6 and 17 s^{-1}. Similar estimates for k_4 can be obtained from the ΔpK_a seen with choline at 0.25 mM oxygen, although in this instance the ΔpK_a might be too small to consider the estimates reliable. The rate of hydride transfer is expected to be similarly affected in the forward (k_3) and reverse (k_4) reactions upon substituting choline with deuterated choline. From the kinetic isotope effect of ∼10 determined for k_3, a rate of less than 2 s^{-1} is therefore estimated for k_4 with 1,2-[$^2H_4$]-choline. Previous kinetic studies showed that k_5 is the same with choline and 1,2-[$^2H_4$]-choline (ref 29). Consequently, a C_r value of ∼0.3 is calculated for the reaction with 1,2-[$^2H_4$]-choline at the lowest oxygen concentration that was used in the experiment, i.e., 0.07 mM. Such a value is expected to yield negligible perturbations of the pH-independent k_{cat}/K_m values and the pK_a values with 1,2-[$^2H_4$]-choline, as was experimentally observed in the k_{cat}/K_m pH profiles with this slow substrate. In principle, estimates of C_r values at different concentrations of oxygen could also be obtained from the pH dependences of the $^D(k_{cat}/K_m)$ values shown in Figure 1, by using eq 7. However, due to error propagation resulting from the kinetic isotope effect data being the ratio of the k_{cat}/K_m values determined with choline to those with 1,2-[$^2H_4$]-choline, each with their associated errors, it is preferable to use the kinetic data from pH profiles, which do not propagate errors. Nonetheless, the pattern with decreasing limiting $^D(k_{cat}/K_m)$ values with decreasing oxygen concentrations experimentally observed (Figure 1) is qualitatively consistent with the conclusions drawn from the analysis of the pH profiles.

(47) The $^D(k_{cat}/K_m)$ and k_{cat}/K_m values with choline and 1,2-[$^2H_4$]-choline are used here for the analysis of the temperature effects because they directly probe the chemical step in which choline is oxidized to betaine aldehyde (ref 29). In contrast, since the k_{cat} value with choline is contributed by both chemical steps of choline and aldehyde oxidation, being equal to $k_3k_7/(k_3 + k_7)$ (ref 29), the temperature effects on the $^Dk_{cat}$ and k_{cat} cannot be ascribed to a single chemical step, thereby preventing a mechanistic interpretation. Nonetheless, the temperature effects on the $^Dk_{cat}$ and the k_{cat} values with choline and 1,2-[$^2H_4$]-choline shown here are qualitatively similar to those observed on the $^D(k_{cat}/K_m)$ and k_{cat}/K_m values, which is at least in agreement with the mechanistic conclusions drawn for the chemical step in which choline is oxidized to betaine aldehyde.

(48) Knapp, M. J.; Klinman, J. P. *Eur. J. Biochem.* **2002**, *269*, 3113−21.

by environmental vibrations of the reaction coordinates other than those affecting the distance between the choline-alkoxide α-carbon and the N(5) atom of the flavin.[18,19,43,48] In agreement with a highly preorganized active site in choline oxidase, small entropies of activation ($\Delta S^{\ddagger}$) are calculated at 25 °C from the experimental data, with values ≤ -0.1 kcal mol^{-1} K^{-1} with both choline and 1,2-[$^2H_4$]-choline. Similar conclusions for environmentally enhanced tunneling of hydrogens at different oxidation states associated with kinetic isotope effects not larger than the values predicted by the semiclassical (bond-stretch) model have also been previously reported for sarcosine oxidase,[17] trimethylamine dehydrogenase,[16] liver alcohol dehydrogenase,[24] and pentaerythriol tetranitrate reductase.[12]

Conclusion

The results of the mechanistic investigation on the effects of oxygen and temperature on the kinetic isotope effects with deuterated choline presented in this study are consistent with the reversible transfer of the hydride in the oxidation of choline occurring quantum mechanically, with the reactive configuration for hydride tunneling being minimally affected by environmental vibrations of the reaction coordinate other than those affecting the distance between the hydride donor and acceptor. This conclusion, along with previously reported mechanistic data,[29,30,36] allows an in-depth description at a molecular level of the catalytic events involved in the oxidation of an alcohol substrate by a flavin-dependent enzyme. Catalysis is triggered by an active site base with a pK_a of 7.5 that removes the hydroxyl proton of the alcohol substrate, with subsequent hydride transfer from the α-carbon of the activated alcohol to the enzyme-bound flavin. The necessary stabilization required for the formation of the choline-alkoxide species is effected through electrostatic interaction with the positively charged side chain of an active site amino acid residue, His_{466}.[36] By decoupling OH and CH bond cleavages,[29] a highly reactive choline-alkoxide species is transiently formed in the active site of the enzyme.[29] Formation of the choline-alkoxide species is also likely to contribute to the correct positioning of the substrate α-carbon, through the electrostatic interaction with His_{466}, for efficient hydride transfer to the flavin. Once both activation and correct positioning of the alcohol substrate have been attained in the enzyme active site, the transfer of the hydride ion from the substrate α-carbon to the flavin will occur quantum mechanically by exploiting the protein dynamical motions that permit a tunneling distance between the substrate α-carbon and the flavin N(5) locus. In this respect, the catalytic strategy for alcohol oxidation employed by choline oxidase has several features in common with that proposed for the zinc-dependent alcohol dehydrogenases, where a positively charged zinc atom in the active site of the enzyme stabilizes a transient alkoxide species from which vibrationally assisted hydride tunneling occurs to the nicotinamide cofactor.[49,50] Thus, there exists the possibility that quantum mechanical hydride tunneling from a "chelated" activated alcohol to an organic cofactor is a common strategy utilized by enzymes that catalyze the oxidation of alcohols to carbonyl compounds, irrespective of the nature of the cofactor.

Acknowledgment. This work was supported in part by Grant PRF #37351-G4 from the American Chemical Society, a Research Initiation Grant (G.G.) and a Molecular Basis Diseases Fellowship from Georgia State University (F.F.). The authors thank Dr. W. W. Cleland for his insightful suggestion of investigating the oxygen dependence of the kinetic isotope effects and the three reviewers for helpful comments and suggestions.

Supporting Information Available: Table S1 shows selected examples of steady-state kinetic data sets with choline or 1,2-[$^2H_4$]-choline as substrate for choline oxidase that were fit with both eqs 1 and 2. Tables S2 and S3 report the measured rate constants and kinetic isotope effects with their related standard deviations for all the data presented in Figures 1 to 4. This material is available free of charge via the Internet at http://pubs.acs.org.

JA0560377

(49) Dworschack, R. T.; Plapp, B. V. *Biochemistry* **1977**, *16*, 2716−25.
(50) Agarwal, P. K.; Webb, S. P.; Hammes-Schiffer, S. *J. Am. Chem. Soc.* **2000**, *122*, 4803−12.